Momentum, Heat, and Mass Transfer for Fixed and Homogeneous Fluidized Beds

The Carman channel model for flow in packed beds is shown to apply for the minimum fluidization velocity and homogeneous fluidized beds. The channel model also provides correlations for mass transfer in the laminar flow region and heat and mass transfer for turbulent flow in a packed bed. Tube bundle data for pressure drop and heat transfer are also evaluated as a packed bed with the channel model.

G. A. HUGHMARK

Ethyl Corporation
Baton Rouge, Louisiana 70821

SCOPE

Analysis of pressure drop for fixed beds and expansion characteristics of fluidized beds have been the subject of many publications. Ergun (1952) presented a literature review for fixed beds and developed an equation (of the friction factor form) for pressure drop with spherical or near spherical particles. Ergun and Orning (1949) and Wen and Yu (1966) analyzed fluidized beds and the minimum fluidization velocity. Extensive experimental data for homogeneous fluidized beds have been presented by Wilhelm and Kwauk (1948) and Richardson and Zaki (1954). Several empirical correlations have been proposed for minimum fluidization and void fraction in expanded fluidized beds. Heat and mass transfer in fixed and fluidized beds have also been areas of interest. Correlations of j factor with Reynolds number have been the most frequent representations of these data.

Carman (1937) utilized the work of Blake (1922) to develop an equation for pressure drop in fixed beds of small particles with the model as flow through parallel tortuous paths. Correlation of experimental data with the friction factor defined by Carman and a Reynolds number with the equivalent channel diameter and actual velocity shows the relation $f = 16/N_{Re}$ for the laminar region. The agreement of this model with pipe flow indicates that it may be useful as a general model for fixed and homogeneous fluidized beds. This work utilizes the channel model for an analysis of pressure drop, heat and mass transfer in fixed and fluidized beds, and heat transfer in tube bundles.

CONCLUSIONS AND SIGNIFICANCE

The channel model proposed by Carman for packed beds appears to apply to both the laminar and turbulent region for packed beds. The model also provides a correlation for the minimum fluidization velocity and for expansion of homogeneous fluidized beds. Laminar flow mass transfer data show that the channel model results in a correlation similar to that for transfer in a circular pipe. Turbulent flow mass and heat transfer data for a packed bed are also correlated with the channel model and appear to correspond to the shear drag in the bed. Mass transfer data for turbulent flow in a fluidized bed indicates a higher transfer rate than in the packed bed. Application of the channel model to tube bundle data indicates that the turbulent region heat transfer-momentum relationship for a bundle with 1.25 equilateral triangular pitch is essentially the same as for the packed bed.

FIXED BEDS—PRESSURE DROP

The Carman equation is:

$$\frac{\Delta P}{L_e} = \frac{2.5 f u_e^2 \rho}{D_e} \tag{1}$$

The velocity u_e is defined as the actual velocity in the packing channels and is represented by the equation:

$$u_e = \frac{u}{\epsilon}\frac{L_e}{L} \tag{2}$$

Carman shows that the ratio L_e/L, the actual length of path taken by the fluid divided by the bed depth, is equal to $\sqrt{2}$.

Experimental pressure drop data for fixed beds are reported by Burke and Plummer (1928), Wilhelm and Kwauk (1948), McConnachie and Thodos (1963), and Wentz and Thodos (1963). These data represent spherical or near spherical particles with air as the fluid. Wilhelm and Kwauk and McCune and Wilhelm (1949) also report data with water as the fluid.

The equivalent diameter for a bed of spherical particles is

$$D_e = 2/3\, D_P \frac{\epsilon}{1-\epsilon} \tag{3}$$

Thus Equations (1), (2), and (3) can be used to obtain a friction factor-Reynolds number relationship for the experimental pressure drop data. Figure 1 shows these data. Agreement is observed for the laminar flow region with turbulence indicated to begin at a Reynolds number of 35. Data for the turbulent region appear consistent and indicate the correlation.

$$f = 1.63/(N_{Re})^{1/3} \tag{4}$$

The Reynolds number of 35 corresponds to a particle Reynolds number $D_P u_e/\nu$ of about 100 for $\epsilon = 0.35$ which is typical for a fixed bed. A bed of spheres could be expected to show flow pattern transitions aproximating those for a single sphere. Garner, Jenson, and Keey (1959) have described these transitions as a function of Reynolds number. At a particle Reynolds number of about 17, a weak toroidal vortex is formed at the rear stagnation point and the vortex gains strength as the Reynolds number increases. Thus, the observed critical Reynolds number from Figure 1 corresponds to a flow condition where turbulence could be expected in a spherical bed.

Combination of Equations (1), (2), and (3) result in the equation

$$\frac{\Delta P}{L} = \frac{10.6 f u_s^2 \rho}{D_P} \frac{(1-\epsilon)}{\epsilon^3}$$

which is of the same form as the equation proposed by Ergun

$$\frac{\Delta P}{L} = \frac{f_k u_s^2 \rho}{D_P} \frac{(1-\epsilon)}{\epsilon^3} \qquad (5)$$

FLUIDIZED BEDS—MINIMUM FLUIDIZATION VELOCITY

Minimum fluidization velocity data are reported by Wilhelm and Kwauk (1948) with air and water as fluids, Wen and Yu (1966) with water as the fluid, and Miller and Logwinuk (1951) with air, helium, carbon dioxide, and ethane as fluids. These data could be expected to fit the friction factor-Reynolds number relationship for fixed beds with

$$\frac{\Delta P}{L} = (\rho_s - \rho)(1-\epsilon) \qquad (6)$$

Figure 2 shows the experimental data with the friction factor relationship from Figure 1. The data are observed to show a reasonable fit with excellent agreement of the Miller and Logwinuk data in the laminar region. This result indicates that the channel model is also applicable to minimum fluidization data.

EXPANDED FLUIDIZED BEDS

The channel model can also be tested with experimental data for expanded homogeneous fluidized beds. Equation (6) applies for these conditions but the Carman ratio $L_e/L = \sqrt{2}$ must be modified to consider the high void fractions in expanded beds. Figure 3 shows an estimate of L_e/L as a function of void fraction for beds of spherical particles. Experimental data are reported by Wilhelm and Kwauk for air and water fluidization, Richardson and Zaki (1954) for water, glycerol-water, and oil fluidization, and Ergun and Orning (1949) for nitrogen, hydrogen, and carbon dioxide. Figure 4 shows these data and again reasonable agreement is observed with the friction factor-Reynolds number relationship obtained from the fixed bed data.

FIXED BED—HEAT AND MASS TRANSFER

The channel model analysis of fixed bed pressure drop data indicates that heat and mass transfer for the laminar

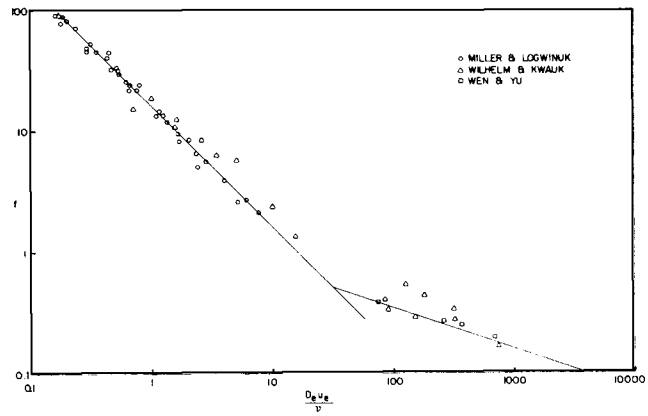

Fig. 2. Minimum fluidization data.

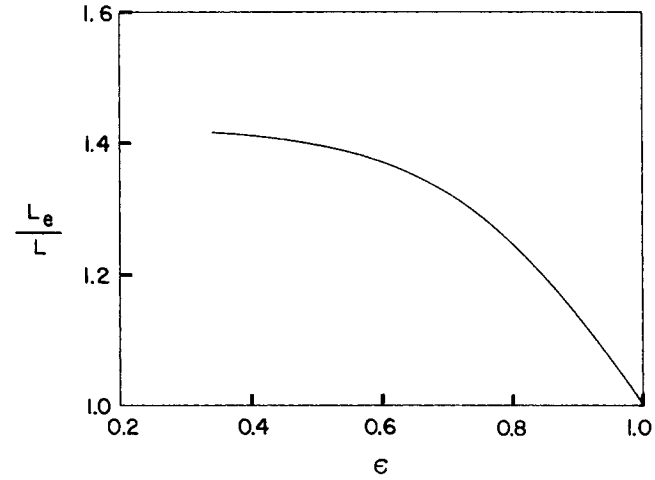

Fig. 3. Actual path length.

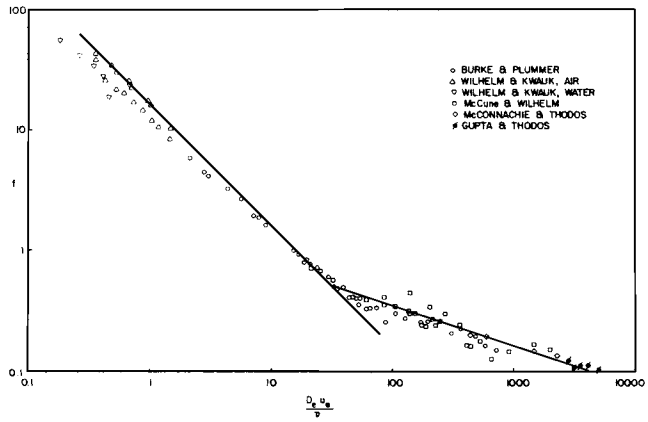

Fig. 1. Packed bed data.

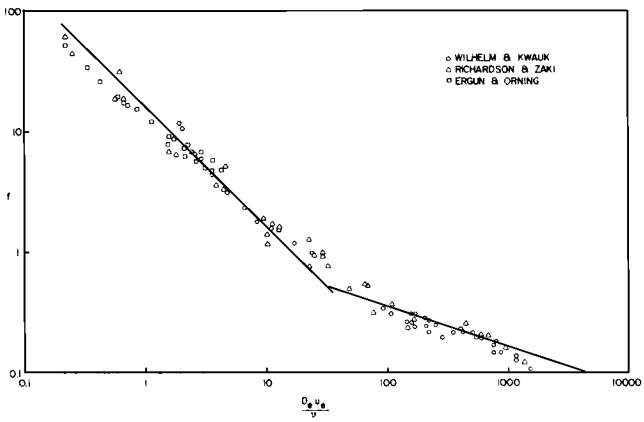

Fig. 4. Fluidized bed data.

flow region may be analogous to that for flow in a pipe. Mass transfer data are available from the work of Williamson, Bazaire, and Geankoplis (1963) for benzoic acid in water, Wilson and Geankoplis (1966) for benzoic acid in water and propylene glycol solutions, and Gaffney and Drew (1950) for salicyclic acid in benzene and succinic acid in n-butanol and aqueous acetone. These data represent a Schmidt number range of 160 to 70,000. Figure 5 shows the data plotted with the Sherwood number as a function of the reciprocal Reynolds and Schmidt number. The correlation indicates that the unity exponent on the Schmidt number is reasonable in accordance with laminar flow theory. Prior correlations with the j factor have indicated exponents of about two-thirds for the Schmidt number but this results from including these data with the data for the turbulent region. Figure 5 also shows the correlation for fully developed parabolic flow in a circular pipe with $L/D = 1$. The correlation of the packed bed data shows the same type of curvature as the pipe correlation. Heat transfer data are not shown with Figure 5 because of the apparent difficulty in obtaining meaningful experimental heat transfer data. Much of the reported experimental data show Nusselt numbers less than unity with the channel model.

Mass transfer data for the turbulent region are reported by Wilke and Hougen (1945) for water in air, McCune and Wilhelm (1949) for 2-napthol in water, McConnachie and Thodos (1963) and Gupta and Thodos (1963) for water in air, and Gaffney and Drew for the three systems listed in the laminar flow discussion. Figure 6 show these data as $N_{Sh}/(N_{Sc})^{1/3}$ versus Reynolds number. The data

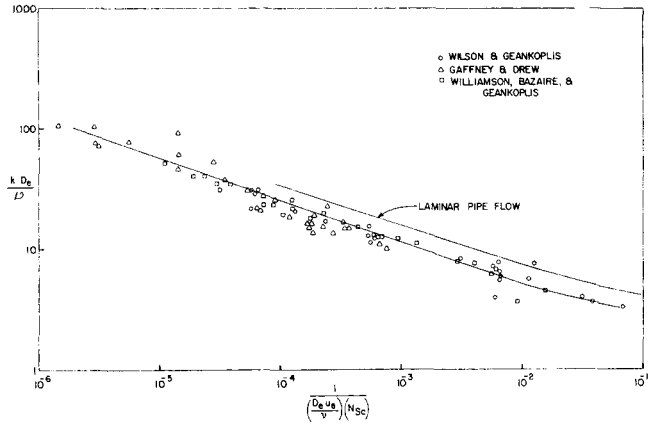

Fig. 5. Laminar mass transfer data.

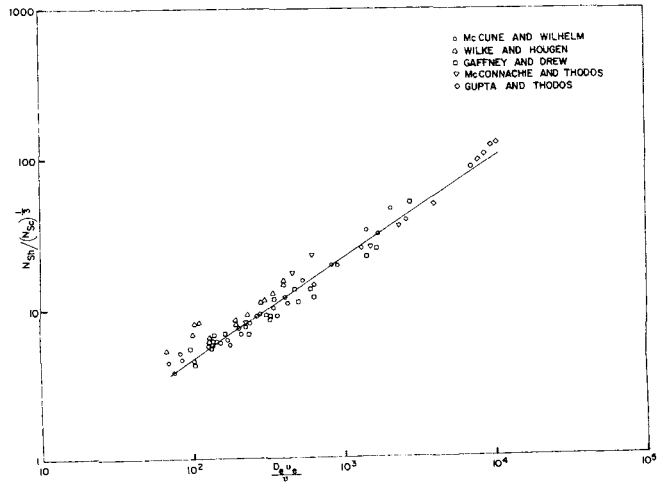

Fig. 6. Fixed bed mass transfer.

represent the Schmidt number range of 0.6 to 10,000. The Schmidt number exponent appears to adequately represent the data. The correlation equation for the data is

$$\frac{k D_e}{\mathcal{D}} = 0.22 \left(\frac{D_e u_e}{\nu} \right)^{2/3} (N_{Sc})^{1/3} \qquad (7)$$

Figure 6 shows only mass transfer data. McConnachie and Thodos and Gupta and Thodos also report heat transfer data. These data are similar to the mass transfer data with respect to the model represented by Equation (7).

The Reynolds analogy for momentum, heat, and mass can be used to estimate the shear drag contribution to friction. For momentum, heat, and mass

$$\frac{f}{2} u_e = \frac{h}{\rho C_P} (N_{Pr})^{2/3} = k (N_{Sc})^{2/3} \qquad (8)$$

Equation 7 can be rearranged to

$$k = 0.22 \left(\frac{\nu}{D_e u_e} \right)^{1/3} (N_{Sc})^{-2/3} \qquad (9)$$

Combination of the two equations yields

$$f = 0.44/(N_{Re})^{1/3}$$

which is 27% of the value obtained from the pressure drop data in Equation (5). The fraction shear drag contribution is also observed to be independent of Reynolds number. Wentz and Thodos (1963) experimentally determined form and total drag for several packed bed configurations. The data for $\epsilon = 0.354$ indicate that shear drag represents about 20% of the total drag for a single sphere at a particle Reynolds number of 1000. The shear drag contribution determined from the momentum-mass transfer data for packed beds appears consistent with these data.

McCune and Wilhelm also report mass transfer data for fluidized beds of 2-napthol particles with water. Figure 7 shows these data. The correlating equation is

$$\frac{k D_e}{\mathcal{D}} = 0.20 \left(\frac{D_e u_e}{\nu} \right)^{3/4} (N_{Sc})^{1/3}$$

Comparison with Equation (9) indicates that mass transfer rates are higher in a fluidized bed than in the fixed bed and that the rate increases more rapidly with Reynolds number than in the fixed bed.

TUBE BUNDLES

The preceding analysis applies the equivalent diameter concept to beds of spherical particles. It is interesting to apply this concept to the experimental data for pressure drop and heat transfer in tube bundles as a fixed bed of cylindrical particles. The equivalent diameter for a tube bundle is

$$D_e = D_t \frac{\epsilon}{1 - \epsilon} \qquad (10)$$

Equations (1), (2), and (10) can then be used to calculate friction factors. Experimental data are reported by Pierson (1937) for air, Omohundro, Bergelin, and Colburn (1949), Bergelin, Brown, Hull, and Sullivan (1950), and Bergelin, Brown, and Doberstein (1952) for oil. Figure 8 shows the turbulent region friction factor data for 1.25 and 1.5 equilateral triangular pitch and 1.25 staggered square pitch. Figure 9 shows the heat transfer data for the three tube layouts. Data for the 1.5 equilateral triangular and 1.25 staggered square pitch are represented by the equation:

$$\frac{h D_e}{k} = 0.31 \left(\frac{D_e u_e}{\nu} \right)^{2/3} (N_{Pr})^{1/3}$$

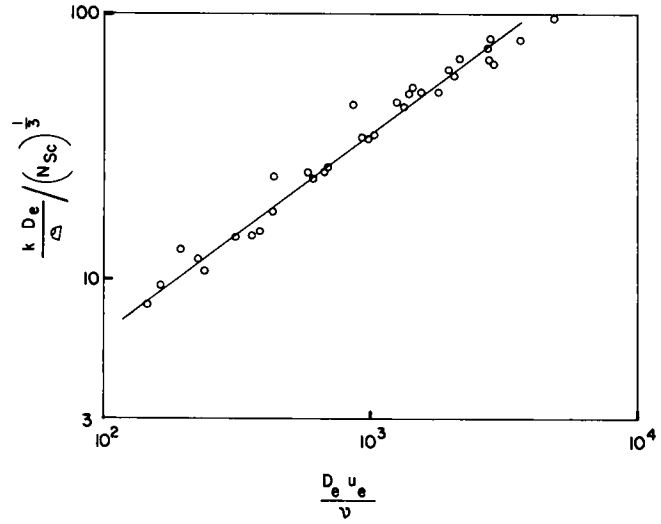

Fig. 7. Fluid bed mass transfer.

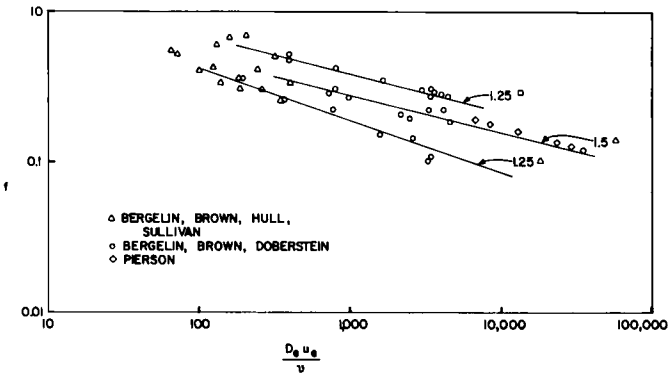

Fig. 8. Tube bundle friction factor.

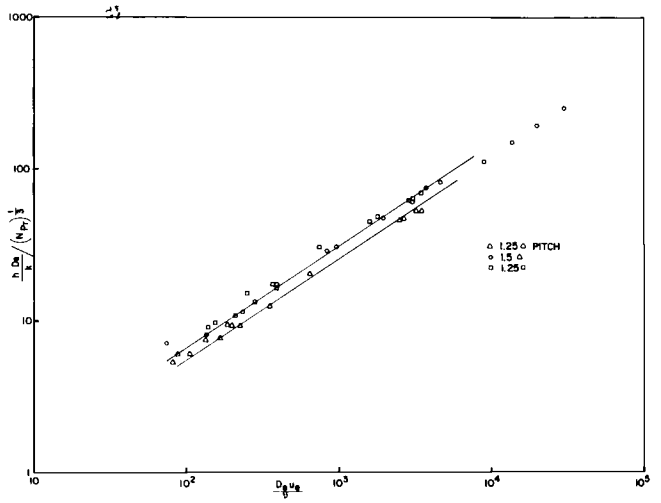

Fig. 9. Tube side heat transfer.

Friction factor data correlations are $f = 1.56/(N_{Re})^{1/4}$ for 1.5 equilateral triangular pitch and $f = 2.17/(N_{Re})^{1/4}$ for 1.25 staggered square pitch. The momentum-heat transfer analogy indicates that shear drag is 22% and 16% of total drag for these tube bundles at $N_{Re} = 1000$. The 1.25 equilateral triangular pitch data indicate the equation:

$$\frac{h\,D_e}{k} = 0.26 \left(\frac{D_e\,u_e}{\nu}\right)^{2/3} (N_{Pr})^{1/3}$$

and the friction factor is shown to be $f = 1.87/(N_{Re})^{1/3}$. This tube spacing indicates that fraction shear drag is 28% and is independent of Reynolds number. Thus, this shear drag relationship appears to be the same as for the spherical packed beds.

NOTATION

C_P = specific heat
D_e = equivalent diameter of channel
D_P = particle diameter
D_t = tube diameter
f = Fanning friction factor
f_k = Ergun friction factor
h = heat transfer coefficient
k = mass transfer coefficient
L = bed depth
L_e = actual length of path taken by fluid in traversing depth, L, of bed
N_{Pr} = Prandtl number
N_{Re} = $D_e\,u_e/\nu$, Reynolds number
N_{Re}' = $D_P\,u_s/\nu$, Reynolds number
N_{Sc} = Schmidt number
ΔP = pressure difference
u_e = actual velocity in packing channels
u_s = superficial velocity

Greek Letters

ϵ = packing void fraction
ν = kinematic velocity
ρ = fluid density
ρ_s = solids density

LITERATURE CITED

Bergelin, O. P., et al., "Heat Transfer and Fluid Friction During Flow Across Banks of Tubes—IV," Trans. ASME, **74**, 953 (1952).

Bergelin, O. P., et al., "Heat Transfer and Fluid Friction During Viscous Flow Across Banks of Tubes—III," *ibid.*, **72**, 881 (1950).

Blake, F. C., "The Resistance of Packing to Fluid Flow," *Trans. Am. Inst. Chem. Engrs.*, **14**, 415 (1922).

Burke, S. P., and W. B. Plummer, "Gas Flow Through Packed Columns," *Ind. Eng. Chem.*, **20**, 1196 (1928).

Carman, P. C., "Fluid Flow Through Granular Beds," *Trans. Inst. Chem. Engrs.*, **15**, 150 (1937).

Ergun, Sabri, "Fluid Flow Through Packed Columns," *Chem. Eng. Progr.*, **48**, 89 (1952).

———., and A. A. Orning, "Fluid Flow through Randomly Packed Columns and Fluidized Beds," *Ind. Eng. Chem.*, **41**, 1179 (1949).

Gaffney, B. J., and T. B. Drew, "Mass Transfer from Packing to Organic Solvents in Single Phase Flow through a Column," *ibid.*, **42**, 1120 (1950).

Garner, F. H., et al., "Flow Pattern Around Spheres and the Reynolds Analogy," *Inst. Chem. Engrs.*, **37**, 191 (1959).

Garner, F. H., and R. D. Suckling, "Mass Transfer from a Soluble Solid Sphere," *AIChE J.*, **4**, 114 (1958).

Gupta, A. S., and George Thodos, "Transitional Behavior for the Simultaneous Mass and Heat Transfer of Gases Flowing Through Packed and Distended Beds of Spheres," *Ind. Eng. Chem. Fundamentals*, **3**, 218 (1964).

McConnachie, J. T. L., and George Thodos, "Transfer Processes in the Flow of Gases Through Packed and Distended Beds of Spheres," *AIChE J.*, **9**, 60 (1963).

McCune, L. K., and R. H. Wilhelm, "Mass and Momentum Transfer in Solid-Liquid Systems," *Ind. Eng. Chem.*, **41**, 1124 (1949).

Miller, C. O., and A. K. Logwinuk, "Fluidization Studies of Solid Particles," *ibid.*, **43**, 1220 (1951).

Pierson, O. L., "Experimental Investigation of the Influence of Tube Arrangement on Convection Heat Transfer and Flow Resistance in Cross Flow of Gases Over Tube Banks," *Trans. ASME*, **59**, 563 (1937).

Omohundro, G. A., et al., "Heat Transfer and Fluid Friction

During Viscous Flow Across Banks of Tubes," *ibid.*, **71**, 27 (1949).
Richardson, J. F., and W. N. Zaki, "Sedimentation and Fluidization," *Trans. Inst. Chem. Engrs.*, **32**, 35 (1954).
Wen, C. Y., and Y. H. Yu, "Mechanics of Fluidization," *Chem. Eng. Progr. Symp. Series No. 62*, **62**, 100 (1966).
Wentz, C. A., and George Thodos, "Total and Form Drag Friction Factors for the Turbulent Flow of Air Through Packed and Distended Beds of Spheres," *AIChE J.*, **9**, 358 (1963).
Wilhelm, R. H. and Mooson Kwauk, "Fluidization of Solid Particles," *Chem. Eng. Progr.*, **44**, 201 (1948).
Wilke, C. R., and O. A. Hougen, "Mass Transfer in the Flow of Gases through Granular Solids Extended to Low Modified Reynolds Number," *Trans. Am. Inst. Chem. Engrs.*, **41**, 445 (1945).
Williamson, J. E., et al., "Liquid Phase Mass Transfer at Low Reynolds Numbers," *Ind. Eng. Chem. Fundamentals*, **2**, 126 (1963).
Wilson, E. J. and C. J. Geankoplis, "Liquid Mass Transfer at Very Low Reynolds Numbers in Packed Beds," *ibid.*, **5**, 9 (1966).

Manuscript received April 5, 1972; revision received May 25, 1972; paper accepted May 25, 1972.

Precipitate Coflotation of Orthophosphate and Fluoride

Orthophosphate and fluoride are simultaneously precipitated from aqueous solution, 5.26×10^{-3} M. in each, by La (III). The precipitates are cofloated by the anionic surfactant sodium laurylsulfate, with optimum flotation at pH 4.0 and a stoichiometric lanthanum concentration based on $LaPO_4$ and LaF_3. Over pH 3.5 to 6.0, better than 95% flotation of the total orthophosphate and precipitated fluoride that are present can be floated at a molar sodium laurylsulfate to orthophosphate plus fluoride ratio of 0.023. At lower sodium laurylsulfate concentrations, the flotation decreases at pH 3.5 and 6.0 compared to pH 4.0-5.0; at pH 4.0, an increase in the La(III) concentration decreases the flotation.

DIBAKAR BHATTACHARYYA
JOHN D. ROMANS
and ROBERT B. GRIEVES

University of Kentucky
Lexington, Kentucky 40506

SCOPE

The removal of a soluble ionic species from aqueous solution followed by concentration in a foam or froth can be accomplished by precipitating the ion, then by adding a surface-active agent to act as a collector-frother, and then by aerating the suspension and floating the precipitate-surfactant particulates to the surface of the suspension. The initial charge of the precipitate has a significant effect on the adsorption (or exchange) of the surfactant on the particles, with the change established either by desorption of one of the ionic species of the solid or by adsorption of ions from solution onto the surface of the crystal. The constituent ions of the precipitate present in solution are preferentially adsorbed over other ions. The surfactant, added as a collector-frother in a flotation process, serves three or more functions: the adsorption (or exchange) of the surfactant on the surfaces of the particles makes the precipitate suitable for gas bubble attachment (the surfactant may also promote aggregation of the precipitate, becoming incorporated in the precipitate structure); interaction between surfactant adsorbed on the particles and "free" surfactant adsorbed at the gas-liquid, bubble interfaces produces bubble attachment to the particles; and "free" surfactant acts as a frother, producing a stable foam, which may be further stabilized by the presence of particulates.

The objective of this work is to investigate experimentally the simultaneous precipitation of orthophosphate and fluoride by lanthanum (La (III)) over an acidic pH range (pH 3.5 to 6.0), followed by coflotation of $LaPO_4$ plus LaF_3 (plus crystals containing both orthophosphate and fluoride) with a single surfactant. The effects of pH, lanthanum concentration, and surfactant concentration are discussed in terms of flotation results, in terms of calculated and experimentally-measured solution concentrations of the ionic species of significance, and in terms of the characteristics of the precipitate particles. Lanthanum has been reported as an orthophosphate precipitant superior to Al (III), Fe (III), and Ca (II) salts (Recht et al., 1971; Leckie and Stumm, 1970; Yuan and Hsu, 1970). In particular, at the same cation to orthophosphate ratios, La (III) has yielded lower soluble orthophosphate concentrations (by as much as three orders of magnitude) over a broader pH range compared to Al (III) (Recht et al., 1971). Precipitation with Ca (II) necessitates an alkaline pH. La (III) also yields a small solubility product with fluoride (Eriksson and Johansson, 1970), although the soluble fluoride concentrations are higher than those of orthophosphate. The precipitation of orthophosphate by Al (III) is influenced by the presence of fluoride (Leckie and Stumm, 1970; Yuan and Hsu, 1971).

Possible applicability of this work is to the treatment of aqueous wastes produced by wet scrubbers used by the phosphoric acid manufacturing industry (Barber and Farr, 1970; Anon., 1970). Both orthophosphate and fluoride can be scrubbed simultaneously from stack emissions by a variety of wet air pollution control devices. However, the under-flow stream from the scrubbers must be treated for phosphate and fluoride removal and possible recovery before discharge to a receiving stream. The 5.26×10^{-3}M. concentrations each of orthophosphate and fluoride used in

Correspondence concerning this paper should be addressed to R. B. Grieves.